Environmental Science & Technology

pubs.acs.org/est

Article

Deciphering Dissolved Organic Matter: Ionization, Dopant, and Fragmentation Insights via Fourier Transform-Ion Cyclotron Resonance Mass Spectrometry

Martin R. Kurek,* Brett A. Poulin, Amy M. McKenna, and Robert G. M. Spencer

Cite This: *Environ. Sci. Technol.* 2020, 54, 16249−16259

Read Online

ACCESS | Metrics & More | Article Recommendations | Supporting Information

ABSTRACT: Fourier transform-ion cyclotron resonance mass spectrometry (FT-ICR MS) has been increasingly employed to characterize dissolved organic matter (DOM) across a range of aquatic environments highlighting the role of DOM in global carbon cycling. DOM analysis commonly utilizes electrospray ionization (ESI), while some have implemented other techniques, including dopant-assisted atmospheric pressure photoionization (APPI). We compared various extracted DOM compositions analyzed by negative ESI and positive APPI doped with both toluene and tetrahydrofuran (THF), including a fragmentation study of THF-doped riverine DOM using infrared multiple photon dissociation (IRMPD). DOM compositions followed the same trends in ESI and dopant-assisted APPI with the latter presenting saturated, less oxygenated, and more N-containing compounds than ESI. Between the APPI dopants, THF-doping yielded spectra with more aliphatic-like and N-containing compounds than toluene-doping. We further demonstrate how fragmentation of THF-doped DOM in APPI resolved subtle differences between riverine DOM that was absent from ESI. In both ionization methods, we describe a linear relationship between atomic and formulaic N-compositions from a range of DOM extracts. This study highlights that THF-doped APPI is useful for uncovering low-intensity aliphatic and peptide-like components in autochthonous DOM, which could aid environmental assessments of DOM across biolability gradients.

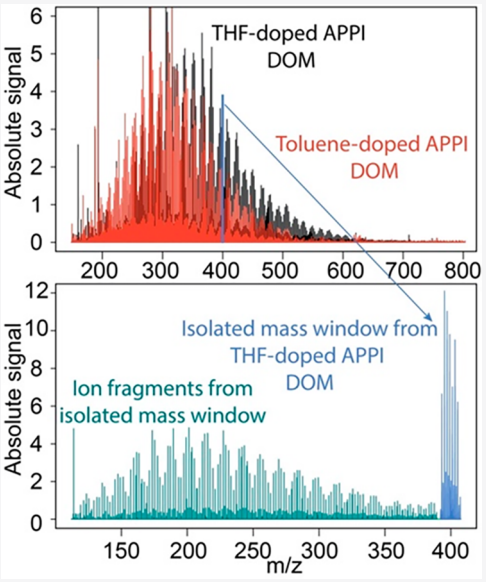

INTRODUCTION

Dissolved organic matter (DOM) is a diverse mixture of organic molecules representing a range of terrestrially derived (allochthonous) and aquatic (autochthonous) compounds that vary along a spectrum of reactivity.[1,2] This spectrum includes biolabile compounds that are prone to biological mineralization, such as saturated and heteroatom-rich molecules, and biostable molecules which are generally more unsaturated and oxygenated.[3−5] Together, these compounds are critical components of the carbon cycle and their characterization has revealed many global physical and environmental processes.[6−8] Fourier transform-ion cyclotron resonance mass spectrometry (FT-ICR MS) has been extensively utilized to characterize thousands of molecules that constitute DOM within a diverse range of aquatic environments.[9−11] Predominantly, DOM analysis has been conducted by negative electrospray ionization (ESI) due to the selective ionization of polar acidic functional groups (e.g., carboxylic acids) and small required sample volumes[12,13] but suppresses ionization of many lower abundance N,S-containing compounds. Furthermore, chromatographic separations suggest that a higher molecular weight and UV-active pool of compounds are excluded from ESI spectra.[14−16] In contrast, atmospheric pressure photoionization (APPI) has been used to ionize nonpolar organic compounds from several environments[17,18] with potential to reveal compounds invisible to ESI that could be important components in aquatic DOM.[19]

Positive APPI FT-ICR MS has been implemented in petroleum analysis due to its nonselective ionization and simultaneous production of both positive and negative ions. In practice, DOM ionization in APPI from direct photon absorption is poor but can be enhanced by a chemical dopant, forming both radicals and protonated ions.[20,21] Numerous studies have utilized toluene as an APPI dopant to ionize a wide range of less polar and aromatic compounds,[21−23] while other dopants such as tetrahydrofuran (THF) have displayed a high efficiency for ionizing S-containing molecules in

Received: August 3, 2020
Revised: October 16, 2020
Accepted: November 5, 2020
Published: November 19, 2020

https://dx.doi.org/10.1021/acs.est.0c05206
Environ. Sci. Technol. 2020, 54, 16249−16259

petroleum.[24,25] Given the differences in ionization energy for toluene and THF (8.83 and 9.40 eV, respectively), as well as polarity (0.375 and 1.750 dipole moment, respectively),[26] the choice of dopant will likely influence the ionization, and therefore, detection of molecules within DOM samples. For instance, given the highly aromatic nature of aquatic DOM compounds,[7,11] toluene has been utilized in APPI analysis of DOM across several samples,[27−30] but still only represents a minor fraction of the total DOM with uncharacterized structures.

Fragmentation studies of organic compounds with FT-ICR MS have been used to probe the dominant features within complex mixtures.[31−33] Most commonly in ESI-DOM analysis, collision induced dissociation (CID) has investigated the functional groups of DOM fractions, revealing series differing by CO_2 and H_2O units originating from highly ionizable carboxylic groups.[34−36] In contrast, infrared multiple photon dissociation (IRMPD), often used in APPI, fragments C−O and C−C bonds, providing more structural information and not solely reflecting the best (carboxyl and hydroxyl) leaving groups.[32,37] Although IRMPD has characterized petroleum mixtures,[31,32] it has scarcely been applied to aquatic DOM,[38] providing a new opportunity to study the structural diversity of DOM, including aquatic heteroatom-containing compounds.

Dissolved organic N (DON) represents an important subset of DOM that indicates land cover,[39−41] microbial processing,[42] and possibly abiotic N incorporation.[43] N-containing compounds are important biolabile components of DOM that are leached into headwaters from cropland or pastures where they sustain further microbial processing of organic matter.[40,41,44] DON is also a major component of wastewater effluent, that if left unmonitored, could contribute to nutrient loading in N-sensitive watersheds.[45]

The inherent complexity of DOM requires multiple analytical dimensions to understand its role within the carbon cycle. Previous studies have probed the compositions of DOM between APPI and ESI,[27,28,46,47] but have either been limited in their compositional scope to a single DOM sample or confined to DON characterization. Additionally, no DOM study, to our knowledge, has utilized dopants other than toluene, which is already selective toward many of the aromatics that are ionized in ESI.[27] Here, we extensively compare the molecular compositions of DOM across a range of autochthonous and allochthonous endmembers ionized in negative ESI and positive APPI. DOM analyzed in APPI was doped with two dopants (toluene, THF) and further characterized using IRMPD fragmentation to reveal functional groups.[33,38] We propose that parallel analysis of DOM using dopant-assisted APPI and ESI, along with IRMPD fragmentation, will offer greater insight into molecular biolability and functional diversity across environmental gradients than using routine ESI analysis alone. Moreover, we hypothesize that THF-doped APPI will provide enhanced sensitivity to detect a different subset of DOM compared to toluene-doped APPI including N- and S-containing compounds, and may be more suitable than toluene for aquatic DOM analysis.

MATERIALS AND METHODS

Study Sites and Sampling Procedures. The Suwannee River, as the source of the International Humic Substances Society (IHSS) Suwannee River Fulvic Acid (SRFA), has a long history as a DOM allochthonous endmember[9,11,28,48] due to its nature as a blackwater ecosystem. The river originates from the peat-rich Okefenokee swamp in Southeast Georgia and discharges into the Gulf of Mexico in North Florida. The Suwannee River is characterized by its acidity, low inorganic ion concentrations, and high relative content of humic and fulvic acids.[48] Sample water was collected at Suwannee River State Park near Ellaville, FL (30°23′08.5″N 83°10′13.9″W) on 10/06/19.

The Kissimmee River is an anthropogenically impacted river in South Florida with its headwaters starting at the Kissimmee Chain of Lakes south of Orlando and draining into Lake Okeechobee. The watershed consists primarily of natural wetlands and floodplains surrounding the river including pasture, citrus, and dairy farmland.[49] The river has been identified as a key source for nutrient loading into Lake Okeechobee from its mixed watershed, further complicated by the effects of stream channelization on the local wetlands since the 1960s.[50] For these reasons it was selected to represent an anthropogenic riverine endmember. Water was collected from site S-65E (27°13′32.0″N 80°57′46.0″W) on 10/06/19.

Wakulla Springs is the largest and deepest freshwater spring in the world serving as the source of the Wakulla River which confluences into the St. Mark's River before emptying into the Gulf of Mexico in the Florida panhandle. The Spring is surrounded by mostly forested karst topography and consists of a network of conduits supplied by groundwater with low DOC and microbial-derived DOM.[42] It was selected to represent an autochthonous endmember and sampled at Sally Ward Spring (30°14′29.8″N 84°18′39.2″W) on 10/02/19.

Water samples (4 L) from the three terrestrial Florida waters were collected into acid-washed polycarbonate bottles using a peristaltic pump and filtered in-line using Nalgene tubing through a 0.45 μm capsule filter before transport to the laboratory in the dark at 4 °C and frozen immediately until analysis.

A suite of organic hydrophobic fraction (HPOA) and fulvic acid (FA) samples were also included in this study, isolated by XAD-8 resin.[51] Samples included: Penobscot River at Eddington (HPOA),[52] Suwannee River (HPOA),[48] Lake Fryxell (FA) from 11m depth,[53] Pacific Ocean surface water (HPOA),[54] and Florida Everglades 2B South (HPOA),[55] representing well-characterized endmember DOM sources. The five isolates were reconstituted in Milli-Q water to a concentration of 10 mg C L^{-1} prior to solid phase extraction on PPL resin and analysis (described in detail below).

Geochemical Analysis. In triplicate, filtered samples were acidified with HCl and analyzed for dissolved organic carbon (DOC) concentration using a Shimadzu TOC-L CPH high temperature catalytic oxidation total organic carbon analyzer (Shimadzu Corp., Kyoto, Japan) with sparging to remove dissolved inorganic C using established methodology.[5,11,42] Chromophoric DOM was measured as the absorbance at 254 nm at room temperature using a Horiba Scientific Aqualog (Horiba Ltd., Kyoto, Japan). The specific UV absorbance at 254 nm ($SUVA_{254}$) was calculated by normalizing the absorbance to the DOC concentration.[56] The total N and C content of the isolates were used to calculate the atomic N/C as determined using a CHN analyzer by Huffman Hazen Laboratories (Golden, CO).

Solid Phase Extraction. All eight DOM samples, including the Florida whole waters and isolates, were acidified (pH 2) and solid phase extracted. Bond-Elut PPL columns (Agilent Technologies Inc., Santa Clara, CA) were used for the

https://dx.doi.org/10.1021/acs.est.0c05206
Environ. Sci. Technol. 2020, 54, 16249−16259

extraction following established protocols.[57] PPL columns were prepared by soaking overnight with methanol, rinsing with methanol once, and rinsing with Milli-Q water at pH 2 twice. For the samples intended for ESI analysis, 40 μg organic C was isolated onto 100 mg 3 mL PPL columns (assuming at least 65% recovery[57]) and eluted with 1 mL of methanol. Organic C for the samples intended for APPI were collected at a higher concentration (750 μg C) onto 1 g 6 mL PPL columns and eluted with 3 mL of methanol. Methanol eluents were collected into precombusted (550 °C, > 4 h) glass vials and stored at −20 °C until analysis. Prior to analysis, APPI samples were treated with an organic dopant to increase ionization efficiency. All APPI samples were diluted with 1-part THF and 4-parts methanol (volume-to-volume; v/v) to a final organic C concentration of 50 μg mL^{-1}. A subset of the extracts was further diluted, due to lower solubility, with 1-part toluene and 9-parts methanol (v/v) to 50 μg mL^{-1} organic C.

FT-ICR MS Analysis. Methanol PPL extracts were analyzed on a custom built 9.4-T FT-ICR MS (Oxford Corp., Oxney Mead, UK) with a 22 cm diameter bore at the National High Magnetic Field Laboratory (Tallahassee, FL).[58] The instrument was optimized for m/z 150−1800, with ion optics (including accumulator, transfer quadrupole), excitation (150−2000 Da with a broadband frequency sweep excitation waveform), and detection (m/z 143). Signal acquisition for each sample were optimized using IHSS SRFA dissolved in methanol according to previous methods[59] with a modular Predator ICR data station.[60] Negatively charged ions from DOM were produced via ESI at a flow rate of 500 nL min^{-1} and collected over 100 coadded scans. Organic C concentrations and flow rates for both dopants in APPI positive were all tested on IHSS SRFA in the range of 50−250 μg C mL^{-1} and 30−100 μL min^{-1} before optimization for the DOM samples. Ions from the doped extracts were produced at atmospheric pressure with an external APPI source (Ion Max APPI source, Thermo-Fisher Scientific, Inc., San Jose, CA) at a flow rate of 30 μL min^{-1}, collected over 100 coadded scans, and internally calibrated based on highly abundant oxygen containing alkylation series with a "walking calibration" equation ($141<m/z<1000$).[61] Mass spectral peaks with signal magnitude greater than six times the baseline root-mean-square noise level were exported to a peak list. Elemental composition assignments were made with PetroOrg©[62] constrained by $C_{4-45}H_{4-92}O_{1-25}N_{0-4}S_{0-2}$ and not exceeding 0.2 ppm error.

Fragmentation experiments were performed using IRMPD on the THF-doped Suwannee and Kissimmee River PPL extracts (50 μg C mL^{-1}) in APPI positive. The isolated mass range of 392−408 Da was collected over 30 coadded scans and then fragmented using a 40 W continuous-wave CO_2 laser (λ = 10 μm; Synrad model J48−2 Mukilteo, WA) for 300−500 ms of irradiation at 50% laser power. Ions were collected over the mass range of 141−391 m/z over 50 coadded scans.

Data Processing and Statistical Analysis. Post processing and statistical analysis of the assigned formulae were done using Microsoft Excel and R using the ggplot2[63] and eulerr[64] packages. Molecular properties such as the double bond equivalence (DBE and DBE/C) and modified aromaticity index (AI_{mod}) were calculated according to Koch and Dittmar[65,66] and the CHO-index (average carbon oxidation state) according to Mann et al.[67] For each formula, the N/C and S/C ratios were calculated as the sum of all N or S atoms divided by the sum of all C atoms.[55] The average formulaic N/C and S/C for a DOM sample were determined by averaging individual N/C and S/C molecular ratios, respectively. Formulae were binned into classes based on their heteroatomic composition (CHO, CHON, CHOS, and CHONS compounds) calculated using both number-weighted averaged formulae and intensity-weighted averaged formulae (relative abundance). Principal Component Analysis (PCA) was conducted on the FT-ICR data to assess the relationships between ionization modes and molecular stoichiometries using the factoextra package in R.[68]

For IRMPD experiments, a wide mass range (392−408 Da) enabled ionization of various compounds differing in aromaticity and heteroatoms. Molecular classes of isolated parent molecules and fragments were subjected to Kendrick mass defect analysis based on homologous series of CH_2, O, H_2, CH_2O, CO_2, and H_2O units[69] to find potential fragmentation patterns in the series. Homologous series length distributions between the Suwannee and Kissimmee River for each Kendrick unit (as means) were compared using the nonparametric Wilcoxon method according to previous studies.[42]

RESULTS AND DISCUSSION

DOM Compositions of Diverse Florida Waters. The range of DOC concentrations and DOM compositions of the sampled Florida waters reflected different sources and biogeochemical processes (Table 1). DOC concentrations were the highest in the Kissimmee River (18.8 mg L^{-1}), followed by the Suwannee River (6.4 mg L^{-1}), and the lowest at Wakulla Springs (2.1 mg L^{-1}, Table 1). Although the Kissimmee River had almost 3 times the organic C concentration as the Suwannee River, they both exhibited comparable $SUVA_{254}$ values (4.30 and 4.34 L mg^{-1}C^{1-}m^{-1}, respectively) suggesting they contain similar amounts of terrestrial aromatic carbon.[56] Similarities between the Suwannee and Kissimmee River DOM were also observed in molecular compositions from negative ESI-FT-ICR MS spectra (hereafter referred to as "ESI") which revealed a similar number of assigned formulae, H/C, and aromaticity (quantified using the AI_{mod}) (Table 1). Heteroatomic content is also consistent between the two rivers which contain primarily CHO-containing molecules and similar formulaic N/C than S/C ratios (Table 1). Notably, Kissimmee River DOM exhibits more molecules with O/C < 0.5 in van Krevelen space than Suwannee River DOM (Figure 1, Supporting Information (SI) Figure S1), suggesting Suwannee River DOM is more oxygenated. Aside from the extent of oxygenation, the ESI spectra did not reveal meaningful compositional differences between Suwannee and Kissimmee River DOM that differentiate natural blackwaters from anthropogenically impacted riverine DOM, probably due to their abundance of highly ionizable carboxylic groups in negative ESI, resulting in ion suppression.[13]

Wakulla Springs DOM, however, is quite distinct from the riverine DOM as it has a much lower $SUVA_{254}$ value (0.99 L mg^{-1}C^{1-}m^{-1}) with less chemodiversity (Table 1). DOM from Wakulla Springs is more saturated, less oxygenated, and contains greater N-content from the formulaic N/C and relative proportion of CHON-containing formulae (Table 1). Both the FT-ICR and optical data suggest Wakulla Springs DOM consists of more autochthonous DOM from a localized source, whereas DOM from the Suwannee and Kissimmee rivers are more allochthonous representing various terrestrial

https://dx.doi.org/10.1021/acs.est.0c05206
Environ. Sci. Technol. 2020, 54, 16249−16259

Table 1. Bulk Chemical and FT-ICR MS-Derived Characteristics of the Suwannee River, Kissimmee River, and Wakulla Springs PPL Extracts[a]

	DOC (mg L^{-1})	$SUVA_{254}$ (L mg^{-1} C^{-1} m^{-1})	assigned formulae	H/C	O/C	mass (Da)	AI_{mod}	DBE/C	formulaic N/C (x1000)	formulaic S/C (x1000)	% CHO	% CHON	%CHOS	%CHONS
Suwannee River	6.4 ± 0.1	4.34	9854	1.04	0.50	498.9187	0.35	0.54	30.1	11.4	41.8 (75.0)	36.8 (16.1)	16.2 (7.73)	5.21 (1.2)
Kissimmee River	18.8 ± 0.1	4.30	9724	1.01	0.46	472.9358	0.39	0.56	29.8	11.7	42.1 (74.0)	35.6 (16.6)	17.3 (8.1)	4.99 (1.2)
Wakulla Springs	2.1 ± 0.1	0.99	8601	1.31	0.43	513.4001	0.19	0.41	39.4	6.5	35.0 (62.7)	51.5 (28.4)	9.18 (7.0)	4.28 (1.8)

[a]DOC is reported as the mean ±1σ analytical standard deviation. H/C, O/C, mass, AI_{mod}, DBE/C, formulaic N/C, and formulaic S/C are all computed means. %CHO, %CHON, %CHOS, and %CHONS values present the percentage of all formulae based on number averages, with intensity-weighted averages (relative abundance) presented in parentheses.

sources such as vegetation, leaf litter, and soil inputs.[11] These observations agree with optical and fluorescence measurements from Wakulla and other clearwater springs within the area[42] as well as various blackwaters and vegetation leachates from North Florida.[5]

Comparing ESI to Dopant-Assisted APPI. While ESI differentiated between autochthonous and allochthonous DOM, few compositional differences between DOM from natural and impacted sources were observed (Table 1). Therefore, the molecular composition of each DOM sample was investigated using positive APPI spectra (hereafter referred to as "APPI"), a method known to enhance ionization of N-containing molecules in DOM using toluene doping.[27,28] THF was also considered as a dopant since it has been shown to ionize many N- and S-containing molecules in APPI from petroleum-affected water[24] but has not yet been applied to DOM analysis. Figure 1 shows the overlap of all compounds ionized in ESI with toluene and THF-doped APPI for three different DOM samples. In all three waters, ESI produced more ions than either THF- or toluene-doped APPI and had the highest proportion of unique ions with some commonality shared with APPI (Figure 1, SI Figure S1). In contrast, toluene- and THF-doped APPI shared more common formulae with each other (>50%), yielding fewer unique compounds compared to ESI (Figure 1; SI Tables S1−S3; Figure S2).

Generally, molecules ionized in toluene-doped APPI were of lower mass, more aliphatic (i.e., higher H/C), with lower O/C ratios than molecules ionized by ESI (SI Tables S1−S3, Figure S2). In agreement with past studies,[27,28] toluene-doped APPI resulted in greater N-content with higher N/C ratios and more CHON formulae than in ESI (Table 1; SI Tables S1−S3). However, the higher relative abundance of heteroatoms in toluene-doped APPI spectra and all shared formulae was restricted to only CHON formulae, whereas S-containing molecules were less effectively ionized given their lower relative abundance of CHOS and S/C (SI Tables S1−S3). Compared to ESI, the THF-doped APPI spectra also yielded greater N-content, higher aliphaticity, as well as lower O/C ratios, mass, and S-content (SI Tables S1−S3; Figure S2). However, the THF-doped samples had lower AI_{mod} values than in ESI suggesting a preferential ionization of more saturated or biolabile DOM. This preferential ionization was even observed between toluene- and THF-doped APPI spectra, where THF ionized DOM with greater N-content and higher H/C ratios while toluene ionized compounds that were lower in mass and more unsaturated (SI Tables S1−S3; Figure S2). Furthermore, within the compounds common between both dopants, THF consistently resulted in higher relative abundances of aliphatic compounds while toluene favored more oxygenated and unsaturated molecules, regardless of the DOM source (SI Figure S2).

In both APPI dopants, DOM from Wakulla Springs was shifted to higher H/C and lower O/C ratios than in the riverine DOM, mirroring the autochthonous signatures from ESI (Table 1; Figure 1). In contrast, Suwannee and Kissimmee River DOM was compositionally similar in all aspects, except in N-content which was higher in Kissimmee River DOM with both dopants (SI Table S1 and S2). Within both APPI-doped spectra, Kissimmee River N-content was also greater in each unique and shared fraction (Figure 1) as well as in the fractions common with ESI (SI Tables S1 and S2), meaning this difference was not just a consequence of the ionization. Indeed,

https://dx.doi.org/10.1021/acs.est.0c05206
Environ. Sci. Technol. 2020, 54, 16249−16259

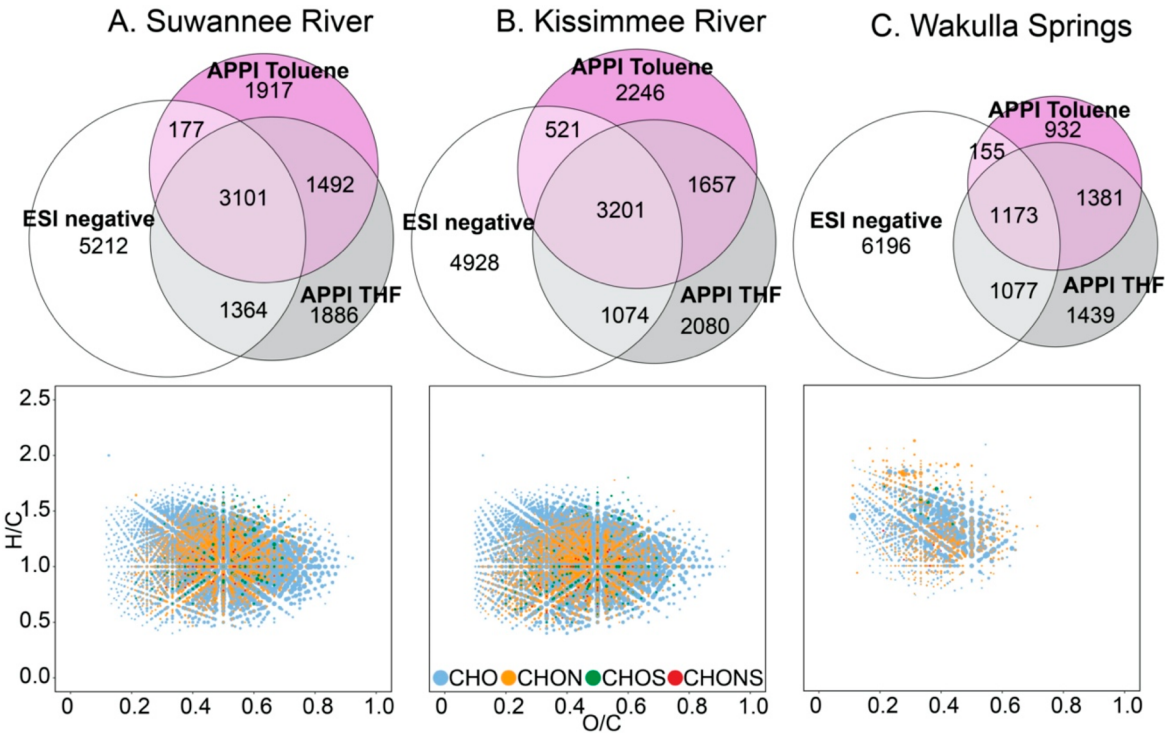

Figure 1. Size-proportional Venn diagrams of the Suwannee River, Kissimmee River, and Wakulla Springs DOM comparing assigned formulae measured in ESI negative, APPI positive with THF doping, and APPI positive with toluene doping. Corresponding van Krevelen diagrams represent all assigned formulae observed using all three ionization approaches; molecular formulae are colored by heteroatom composition (blue = CHO, orange = CHON, green = CHOS, red = CHONS) with the sizes scaled to relative abundances.

APPI ionization suggests Kissimmee River DOM contains more dissolved organic N than Suwannee River DOM and less oxygenated compounds, most likely representing DOM sourced from agricultural practices that leached into the river.[39,41,70] Agricultural DOM has been shown to be highly biolabile with great potential for downstream microbial processing[41,71] and in the case of the Kissimmee River basin, may contribute to the ecological imbalance of eutrophic Lake Okeechobee.

Understanding DOM Functionality with Fragmentation. Traditional analysis of DOM in ESI offers thousands of molecular formulae but does not provide structural information, unless CID fragmentation is utilized to infer functional groups from specific parent ions.[34−36] Here we fragmented THF-doped Suwannee and Kissimmee River DOM samples in APPI using IRMPD to investigate possible molecular features while comparing their molecular compositions. Although we could not determine the exact precursor molecule for each fragment using IRMPD, we provide a robust description of potential series differing by exact chemical units to infer functional groups of the isolated ion distributions. Precursor ions were isolated from 392 to 408 Da and classified according to their molecular compositions (SI Table S4). Within this narrow mass range, both DOM samples contained a nearly equal number of assigned formulae, but Kissimmee River DOM contained a greater relative abundance of CHON compounds than Suwannee River DOM (27% vs 17%, respectively) (SI Table S4; Figure S3A,B). Within each sample, fragments from 141 to 391 Da contained similar molecular class distributions to the precursor ions (SI Table S4) and a Gaussian pattern similar to DOM, except for Suwannee River DOM which had abundant higher masses (Figure 2A). The fragments spanned van Krevelen space similar to each other centered on lower H/C and O/C ratios than the original DOM, suggesting that fragmentation produced resolvable patterns across C−H and C−O bonds (Figure 2C,D). Many of these patterns occur naturally in the environment from biological processing and photochemistry as the majority of the fragment ions in each sample (86%) were also present in the original spectra. Although IR fragmentation and photolysis both cleave C−C bonds, these fragmentation patterns were unlikely due to the same mechanism causing photolysis of aromatic rings since this would produce more saturated compounds[7] and IRMPD fragmentation at longer wavelengths (10 μm) primarily cleaves C−O linkages[37] as well as alkyl and cycloalkyl bonds while retaining aromatic cores intact.[32]

The DOM molecular fragments from the Suwannee and Kissimmee rivers thus represent subunits of their precursor molecules with mass defects that can be used to infer chemical features of homologous series.[69] CHO-containing molecules from the fragments and precursors mostly consisted of homologous series differing by H_2, CH_2, and O series with less from decarboxylation (CO_2) and dehydration (H_2O) series (Figure 2B), in contrast to CID fragmentation studies.[34−36] The same trends persisted in the CHON-containing molecules, but with shorter series lengths (Figure 2C), implying that the primary DOM functional groups from this mass window distribution include alkyl chains and noncarboxylic double bonds. Despite their differing sources, DOM functionalities in both rivers were largely the same with no significant differences (α = 0.05) in Kendrick series distributions between the samples in the CHO and CHON classes. Even within the CHON class, molecules were further

https://dx.doi.org/10.1021/acs.est.0c05206
Environ. Sci. Technol. 2020, 54, 16249−16259

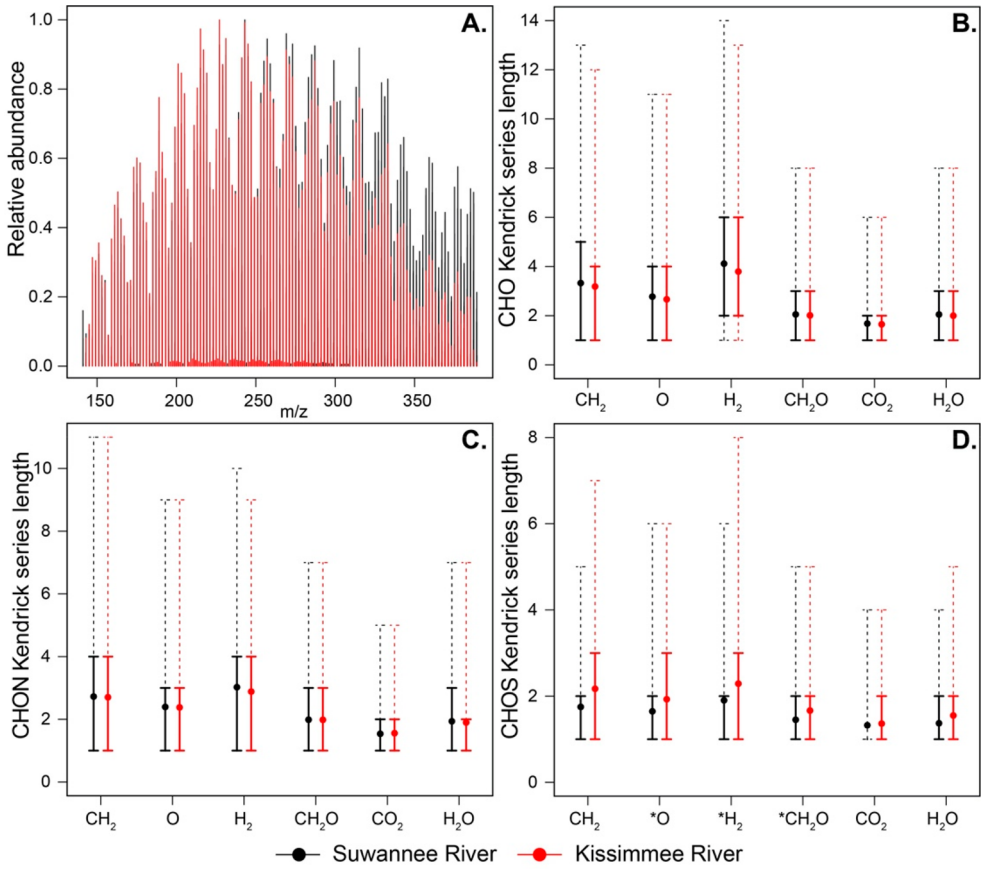

Figure 2. Results from IRMPD experiments of isolated masses at 392−408 Da from the Suwannee River DOM (black) and Kissimmee River DOM (red). (A) Mass spectrum of fragments (141−391 Da) scaled to relative abundances. Boxplots of CH_2, O, H_2, CH_2O, CO_2, and H_2O-based Kendrick series lengths of the two riverine DOM samples is shown for (B) CHO-containing, (C) CHON-containing, and (D) CHOS-containing formulae. Asterisks (*) on *x*-axis labels indicate a significant difference in series means between the two DOM samples (α = 0.05).

subdivided by their N-content ($CHON_1$, $CHON_2$, $CHON_3$) and did not differ between the two samples even though Kissimmee River fragments had higher abundance- and number-based N-content (SI Figure S4, Table S4). In contrast, CHOS-containing series did differ significantly between the two DOM sources with Kissimmee containing longer H_2, O, and CH_2O Kendrick series (Figure 2D) and almost twice as many CHOS fragments (SI Table S4). We interpret the elevated CHOS assignments in Kissimmee River DOM to be a result of sulfurization reactions from agricultural sulfur applications, as has been demonstrated in South Florida.[55]

These data suggest APPI ionizes more molecules with alkyl and unsaturated features in both riverine DOM samples, contrasting the high ionization efficiency of oxygenated and carboxylic groups seen in negative ESI spectra.[13] Additionally, the high similarity of fragments with each other and with their precursor spectra provides further evidence for a universal cascade of reaction pathways responsible for shaping DOM, as was suggested across a larger aquatic gradient.[33] This means that despite the differences in DOM sources between the rivers, downstream transport resulted in a similar degradation pattern of high-abundance CHO and CHON molecules. In contrast, the Kissimmee River DOM composition was distinct in the presence of CHOS molecules, which are normally low in abundance but have been attributed to anthropogenic origins[39,71] and/or abiotic S incorporation.[43,55] These results illustrate the ability of low-abundance ions to differentiate between DOM signatures of terrestrial origins.

Endmember Compositions and Atomic Gradients. The DOM isolates represent a variety of well-characterized autochthonous and allochthonous endmembers with a range of atomic N compositions and stoichiometric ratios in ESI consistent from previous studies (SI Table S5; ref 11). To further evaluate the novel information gained from APPI spectra, we compared the ESI and THF-doped APPI spectra of the DOM isolates (SI Table S5). The THF-doped APPI DOM isolates differed in composition from their ESI spectra (e.g., higher H/C, lower O/C, lower aromaticity, greater N-content, lower mass; SI Table S5), similar to the way Florida DOM differed between THF-doped APPI and ESI (SI Tables S1−S3). Molecular compositions of allochthonous endmembers (Suwannee River, Penobscot River, Everglades) exhibited greater changes in H/C and aromaticity in APPI versus ESI compared to the autochthonous samples (Lake Fryxell FA and Pacific Ocean HPOA) (SI Table S5). The shift to more saturated van Krevelen space in APPI was likely due to reduced ionization of terrestrial aromatic compounds compared to ESI, which are normally abundant in ESI and more unsaturated,[11] in contrast to autochthonous DOM which is naturally more aliphatic.[2]

PCA was conducted on the diverse suite of DOM isolates and Florida waters to visualize the compositional differences of ESI and APPI (THF- and toluene-doped) across a broader framework of aquatic endmembers (Figure 3). Components 1 (PC1) and 2 (PC2) together explain 83% of the variance between the samples using bulk properties derived from the

https://dx.doi.org/10.1021/acs.est.0c05206
Environ. Sci. Technol. 2020, 54, 16249−16259

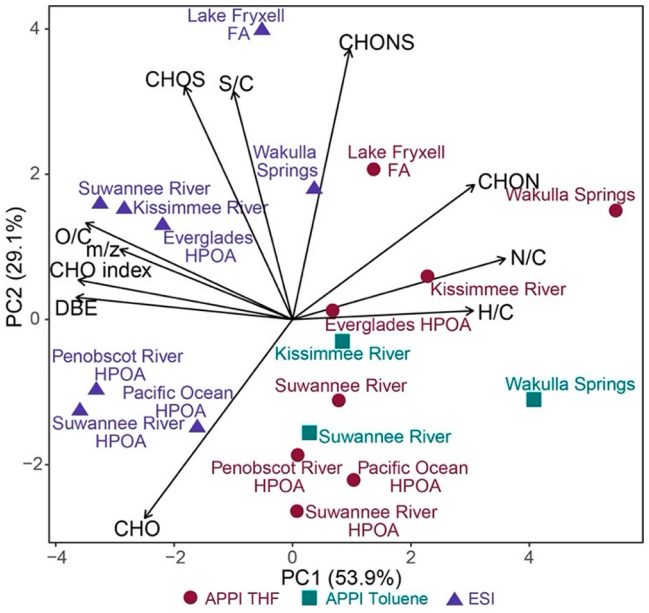

Figure 3. Principal component analysis biplot of DOM samples ionized in ESI negative (blue triangles), THF-doped APPI positive (magenta circles), and toluene-doped APPI positive (green squares). Variables from the FT-ICR spectra are represented by black vectors. HPOA refers to hydrophobic fraction DOM isolates while FA refers to fulvic acid DOM isolates, respectively.

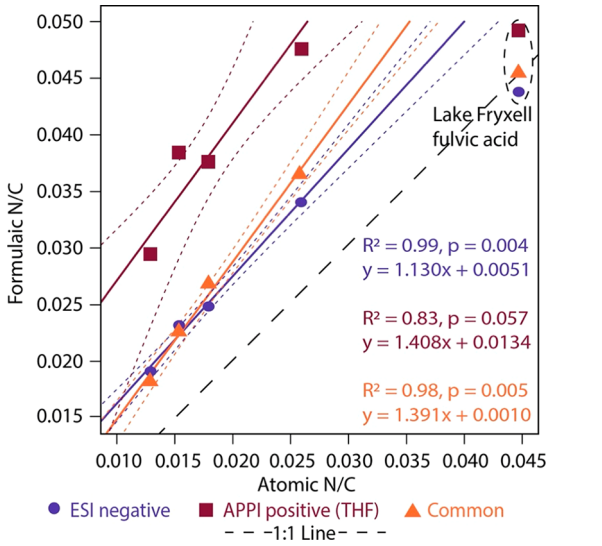

Figure 4. Relationship between the measured atomic N/C of the DOM isolates and the number-averaged formulaic N/C from the FT-ICR spectra measured by ESI negative (blue circles), THF-doped APPI positive (magenta squares), and formulae common to both ionization modes (orange triangles). Linear regressions (colored solid lines) and 95% confidence intervals (colored dashed lines) from each ionization were modeled, omitting the Lake Fryxell fulvic acid sample. The black dashed line denotes the 1:1 line.

mass spectra. There was a clear separation of samples in ESI (blue) and APPI (green represents toluene-doped; magenta represents THF-doped) along PC1 which had strong positive correlations with H/C, N/C, %CHON and was negatively correlated with O/C, DBE, and CHO-index (Figure 3; SI Table S6). In contrast, PC2 revealed a gradient between samples correlating positively with S-content (S/C, %CHOS, and %CHONS) and negatively with %CHO (Figure 3; SI Table S6). This gradient follows DOM compositional differences associated with biolability,[72] separating biolabile microbial DOM from stable and highly processed marine DOM.[73] Although hydrophobic acids are generally less biodegradable,[3] the Everglades HPOA clustered with the Florida DOM rather than the riverine DOM (Suwannee and Penobscot HPOA), illustrating the high N- and S-content present within the region.[55] Furthermore, the separation of riverine DOM isolates from the Florida rivers reflects the compositional differences between DOM retained in XAD-8 (HPOA) and PPL resins,[74] though procedural fractionation was minimized by extracting all samples with PPL prior to analysis. Regardless of the DOM isolation method, the data shows that across a broad range of DOM sources, the greatest amount of variance can be explained by ionization mode alone (ESI vs APPI) while still maintaining a consistent gradient of inferred biolability within each ionization approach. This is further supported by considering the toluene-doped APPI spectra (green) which grouped more closely to the THF-doped spectra (magenta) (i.e., lower PC1 and PC2) rather than clustering separately (Figure 3).

An advantage of APPI over ESI is the additional compositional coverage gained in DON,[28−30,75] though it has not been quantitatively compared to the total atomic N-content. Using the atomic and formulaic N/C ratios from the DOM isolates (SI Table S5), we report a monotonically increasing relationship between total organic N (atomic N/C) and FT-ICR-ionized organic N (formulaic N/C) across a globally diverse range of DON (Figure 4; ref 11). This relationship is consistent for samples measured by ESI (blue), THF-doped APPI (magenta), and ions common between the two approaches (orange) (Figure 4). Applying a linear regression to all samples revealed statistically significant slopes ($\alpha = 0.05$) in all series except for the THF-doped APPI DOM (SI Figure S5), which improved after removing Lake Fryxell from the regression (Figure 4). All regressions plotted above the 1:1 line with slopes slightly greater than unity, suggesting an overestimation of organic N from the formulaic N/C (Figure 4), in contrast to Poulin et al., who reported an underestimation of formulaic S/C with a similar relationship.[55] This overestimation could partly be due to the extraction procedure with PPL retaining a high proportion of extractable organic N compounds[57,74] and subsequent ionization of the concentrated compounds. This is expected to be the case in APPI which ionizes nonpolar, N-containing compounds more effectively than ESI.[28] While both ionization modes increase in formulaic N/C across a gradient of organic N, ESI is more representative because the slope is closer to unity and the intercept is closer to the origin (Figure 4). Indeed, the larger intercept in THF-doped APPI relative to ESI confirms that APPI ionizes an additional set of organic N compounds that are inaccessible during routine ESI-FT-ICR analysis (Figure 1). This is supported by the overlap of the ESI and common ion regressions, showing that formulaic N-content detected by ESI and APPI is conserved in APPI spectra and also increases linearly with atomic N-content (Figure 4).

Although Lake Fryxell DOM is entirely biogenic, the formulaic and atomic N/C relationship was closer to the 1:1 line and did not match other DOM isolates (Figure 4), which is likely explained by its source and isolation procedure. Lake Fryxell is the only fulvic acid extract from the isolates giving it a

https://dx.doi.org/10.1021/acs.est.0c05206
Environ. Sci. Technol. 2020, 54, 16249−16259

different chemical composition than the hydrophobic acids which contain both fulvic and humic acids.[51] One of these differences is that fulvic acids have a lower average N-content than humic acids and DOM,[2] shifting the extracts to lower N/C ratios and introducing less N-containing ions into the instrument. The Antarctic lake is also a "true" autochthonous endmember, composed of biolabile microbial DOM[11,76] and permanently covered by ice, receiving no input from terrestrial vegetation or soil.[51] While the Pacific Ocean HPOA isolate is also considered autochthonous, marine surface DOM does have some terrestrial influence, although many of these signatures are highly processed and degraded.[77] Therefore, the linear relationship of atomic and formulaic N/C in Figure 4 represents organic N that has had some influence from terrestrial sources, and we hypothesize that a similar linear relationship exists for fulvic acids as well as other "true" autochthonous DOM sources with differing slopes from Figure 4 (e.g., groundwater, glaciers, hypersaline lakes). Although regression equations may differ between aquatic environments and different sources,[78] patterns such as in Figure 4 and in Poulin et al.[55] demonstrate the potential of FT-ICR spectra to provide quantitative relationships across environmental gradients with high applicability to targeted studies.

Perspectives and Recommendations. This detailed analysis of DOM ionized in ESI and APPI suggests the overall compositional trends within the scope of diverse endmembers remain largely the same (Figure 1). Although both ionization modes overestimate N-content, formulaic N/C increases linearly with atomic N/C (Figure 4) and we suspect a closer 1:1 relationship may be achieved through different extraction procedures. Between the two dopants tested (toluene and THF), THF-doped APPI provides greater molecular diversity and ionization of organic N while containing many of the same formulae as toluene-doped APPI (Figure 1, SI Tables S1−S3). While both dopants are miscible with methanol, THF is also miscible with water, allowing extra flexibility to directly dope THF into DOM subsets dissolved in water for FT-ICR analysis prior to infusion. Therefore, we recommend doping DOM with THF when analyzing in APPI. In all cases, the common ions between APPI and ESI displayed identical chemical trends to ESI, indicating good agreement between the two methods, but ESI produced more total and unique formulae than either APPI doping method (Figure 1, SI Tables S1−S3, Table S5). In addition, APPI ionized fewer S-containing compounds than in ESI (SI Table S5), contrary to THF-doped petroleum.[24,25] However, a clear advantage of APPI over ESI is the number and diversity of DON and aliphatic-like compounds that were detected (SI Figure S2, Tables S1−S3, Table S5, Figure 4) revealing compositional differences between the Suwannee and Kissimmee Rivers that were indistinguishable in routine ESI analysis (Figure 3) and providing another analytical dimension to DOM analysis.

Realistically, DOM analysis is time and resource-intensive necessitating the highest resolution possible per unit time spent. Therefore, due to the larger sample volumes and higher extraction concentrations needed for APPI to obtain results that corroborate with ESI (Figure 1), we recommend ionization in ESI for all routine analyses. An exception would be for DOM containing uncharacterized DON compounds as well as saturated molecules, such as in highly autochthonous samples,[11] permafrost thaw,[79] or anthropogenically impacted streams which have increased proportions of N-containing formulae due to heightened microbial activity.[39−41] Greater ionization of these compounds through APPI would provide improved sensitivity in bioincubation studies of anthropogenically impacted DOM, where these compounds are typically the most biolabile yet poorly ionized in ESI.[44] APPI analysis could also be beneficial in wastewater DOM analysis to monitor the effects of secondary treatment on removing saturated and peptide-like compounds and assessing needs for advanced treatment.[80] Even after advanced treatment is implemented, further analysis of wastewater effluent could be used to assess DOM biolability as it can be highly reactive in bioassays and contribute to N-loading in local watersheds.[45] Furthermore, when DOM samples are compositionally similar in ESI but require a more detailed comparison to resolve subtle differences (e.g., Suwannee and Kissimmee River DOM; Figure 2), APPI should be considered post hoc in addition to IRMPD fragmentation of selected mass windows. These combined approaches may provide structural information and reactivity pathways that are often unavailable in routine ESI analysis and are even more descriptive than CID fragmentation, potentially deciphering another aspect of DOM complexity.

■ ASSOCIATED CONTENT

Supporting Information

The Supporting Information is available free of charge at https://pubs.acs.org/doi/10.1021/acs.est.0c05206.

FT-ICR MS properties of the FL DOM samples in APPI positive doped with THF and toluene (Tables S1−S3), FT-ICR MS molecular class relative compositions for IRMPD experiments in THF-doped APPI positive (Table S4), FT-ICR MS properties of the DOM isolates in ESI negative and APPI positive doped with THF (Table S5), correlations and percent contributions from variables in the Figure 3 PCA (Table S6), van Krevelen diagrams separated by molecular class from Figure 1 (Figure S1), van Krevelen diagrams of the FL DOM samples comparing between APPI-doped THF and toluene (Figure S2), van Krevelen diagrams of molecular classes from IRMPD experiments in THF-doped APPI positive (Figure S3), Kendrick mass defect boxplots of N-containing classes from IRMPD experiments in THF-doped APPI positive samples (Figure S4), linear regressions between formulaic and atomic N/C content of the DOM isolates including Lake Fryxell FA (Figure S5) (PDF)

■ AUTHOR INFORMATION

Corresponding Author

Martin R. Kurek − *National High Magnetic Field Laboratory Geochemistry Group and Department of Earth, Ocean, and Atmospheric Science, Florida State University, Tallahassee, Florida 32306, United States;* orcid.org/0000-0002-6904-5253; Email: mrk19f@my.fsu.edu

Authors

Brett A. Poulin − *U.S. Geological Survey, Water Mission Area, Boulder, Colorado 80303, United States; Department of Environmental Toxicology, University of California Davis, Davis, California 95616, United States;* orcid.org/0000-0002-5555-7733

Amy M. McKenna − *National High Magnetic Field Laboratory Ion Cyclotron Resonance Facility, Tallahassee,*

Florida 32310, United States; orcid.org/0000-0001-7213-521X

Robert G. M. Spencer − *National High Magnetic Field Laboratory Geochemistry Group and Department of Earth, Ocean, and Atmospheric Science, Florida State University, Tallahassee, Florida 32306, United States*

Complete contact information is available at: https://pubs.acs.org/10.1021/acs.est.0c05206

Notes

The authors declare no competing financial interest.

■ ACKNOWLEDGMENTS

We thank Kenna Butler (USGS) for assistance in the isolation of the DOM and George Aiken for collecting DOM throughout his career—his legacy lives on in many ways including through these DOM isolates. Any use of trade, product, or firm names is for descriptive purposes only and does not imply endorsement by the U.S. Government. A portion of this work was performed in the Ion Cyclotron Resonance User Facility at the National High Magnetic Field Laboratory, which is supported by the National Science Foundation Division of Chemistry and Division of Materials Research through DMR 16-44779, and the State of Florida. We thank Evelyn Becerra for assistance with sampling, Gregory T. Blakney for data processing, John Paul Quinn for maintenance of the 9.4 T passive FT-ICR MS system, and Sydney Niles for helpful discussions.

■ REFERENCES

(1) Aiken, G. R.; Hsu-Kim, H.; Ryan, J. N. Influence of dissolved organic matter on the environmental fate of metals, nanoparticles, and colloids. *Environ. Sci. Technol.* **2011**, *45* (8), 3196−3201.

(2) Perdue, E. M.; Ritchie, J. D. 7.8 - Dissolved organic matter in freshwaters. In *Treatise on Geochemistry*, 2nd ed.; Elsevier Science: Oxford, UK, 2014; pp 237−272.

(3) Wickland, K. P.; Neff, J. C.; Aiken, G. R. Dissolved organic carbon in Alaskan boreal forest: Sources, chemical characteristics, and biodegradability. *Ecosystems* **2007**, *10* (8), 1323−1340.

(4) D'Andrilli, J.; Cooper, W. T.; Foreman, C. M.; Marshall, A. G. An ultrahigh-resolution mass spectrometry index to estimate natural organic matter lability. *Rapid Commun. Mass Spectrom.* **2015**, *29* (24), 2385−2401.

(5) Textor, S. R.; Guillemette, F.; Zito, P. A.; Spencer, R. G. M. An Assessment of Dissolved Organic Carbon Biodegradability and Priming in Blackwater Systems. *J. Geophys. Res.: Biogeosci.* **2018**, *123* (9), 2998−3015.

(6) Spencer, R. G.; Aiken, G. R.; Wickland, K. P.; Striegl, R. G.; Hernes, P. J. Seasonal and spatial variability in dissolved organic matter quantity and composition from the Yukon River basin, Alaska. *Global Biogeochemical Cycles* **2008**, *22* (4), 1−13.

(7) Stubbins, A.; Spencer, R. G.; Chen, H., Hatcher, P. G.; Mopper, K.; Hernes, P. J.; Six, J. Illuminated darkness: Molecular signatures of Congo River dissolved organic matter and its photochemical alteration as revealed by ultrahigh precision mass spectrometry. *Limnol. Oceanogr.* **2010**, *55*(4), 1467−1477.

(8) Niu, X. Z.; Harir, M.; Schmitt-Kopplin, P.; Croué, J. P. Characterisation of dissolved organic matter using Fourier-transform ion cyclotron resonance mass spectrometry: Type-specific unique signatures and implications for reactivity. *Sci. Total Environ.* **2018**, *644*, 68−76.

(9) Hertkorn, N.; Ruecker, C.; Meringer, M.; Gugisch, R.; Frommberger, M.; Perdue, E. M.; Schmitt-Kopplin, P. High-precision frequency measurements: indispensable tools at the core of the molecular-level analysis of complex systems. *Anal. Bioanal. Chem.* **2007**, *389*(5), 1311−1327.

(10) Gonsior, M.; Peake, B. M.; Cooper, W. T.; Podgorski, D. C.; D'Andrilli, J.; Dittmar, T.; Cooper, W. J. Characterization of dissolved organic matter across the Subtropical Convergence off the South Island, New Zealand. *Mar. Chem.* **2011**, *123* (1−4), 99−110.

(11) Kellerman, A. M.; Guillemette, F.; Podgorski, D. C.; Aiken, G. R.; Butler, K. D.; Spencer, R. G. Unifying concepts linking dissolved organic matter composition to persistence in aquatic ecosystems. *Environ. Sci. Technol.* **2018**, *52* (5), 2538−2548.

(12) Sleighter, R. L.; Hatcher, P. G. The application of electrospray ionization coupled to ultrahigh resolution mass spectrometry for the molecular characterization of natural organic matter. *J. Mass Spectrom.* **2007**, *42* (5), 559−574.

(13) Ohno, T.; Sleighter, R. L.; Hatcher, P. G. Comparative study of organic matter chemical characterization using negative and positive mode electrospray ionization ultrahigh-resolution mass spectrometry. *Anal. Bioanal. Chem.* **2016**, *408* (10), 2497−2504.

(14) These, A.; Reemtsma, T. Limitations of electrospray ionization of fulvic and humic acids as visible from size exclusion chromatography with organic carbon and mass spectrometric detection. *Anal. Chem.* **2003**, *75* (22), 6275−6281.

(15) Piccolo, A.; Spiteller, M.; Nebbioso, A. Effects of sample properties and mass spectroscopic parameters on electrospray ionization mass spectra of size-fractions from a soil humic acid. *Anal. Bioanal. Chem.* **2010**, *397* (7), 3071−3078.

(16) Hawkes, J. A.; Sjöberg, P. J.; Bergquist, J.; Tranvik, L. J. Complexity of dissolved organic matter in the molecular size dimension: insights from coupled size exclusion chromatography electrospray ionisation mass spectrometry. *Faraday Discuss.* **2019**, *218*, 52−71.

(17) Barrow, M. P.; Witt, M.; Headley, J. V.; Peru, K. M. Athabasca oil sands process water: Characterization by atmospheric pressure photoionization and electrospray ionization Fourier transform ion cyclotron resonance mass spectrometry. *Anal. Chem.* **2010**, *82* (9), 3727−3735.

(18) Barrow, M. P.; Peru, K. M.; Fahlman, B.; Hewitt, L. M.; Frank, R. A.; Headley, J. V. Beyond naphthenic acids: environmental screening of water from natural sources and the Athabasca oil sands industry using atmospheric pressure photoionization Fourier transform ion cyclotron resonance mass spectrometry. *J. Am. Soc. Mass Spectrom.* **2015**, *26* (9), 1508−1521.

(19) Mopper, K.; Stubbins, A.; Ritchie, J. D.; Bialk, H. M.; Hatcher, P. G. Advanced instrumental approaches for characterization of marine dissolved organic matter: extraction techniques, mass spectrometry, and nuclear magnetic resonance spectroscopy. *Chem. Rev.* **2007**, *107* (2), 419−442.

(20) Robb, D. B.; Covey, T. R.; Bruins, A. P. Atmospheric pressure photoionization: an ionization method for liquid chromatography−mass spectrometry. *Anal. Chem.* **2000**, *72* (15), 3653−3659.

(21) Robb, D. B.; Blades, M. W. State-of-the-art in atmospheric pressure photoionization for LC/MS. *Anal. Chim. Acta* **2008**, *627* (1), 34−49.

(22) Purcell, J. M.; Hendrickson, C. L.; Rodgers, R. P.; Marshall, A. G. Atmospheric pressure photoionization Fourier transform ion cyclotron resonance mass spectrometry for complex mixture analysis. *Anal. Chem.* **2006**, *78* (16), 5906−5912.

(23) Purcell, J. M.; Hendrickson, C. L.; Rodgers, R. P.; Marshall, A. G. Atmospheric pressure photoionization proton transfer for complex organic mixtures investigated by Fourier transform ion cyclotron resonance mass spectrometry. *J. Am. Soc. Mass Spectrom.* **2007**, *18* (9), 1682−1689.

(24) Ajaero, C.; Peru, K. M.; Hughes, S. A.; Chen, H.; McKenna, A. M.; Corilo, Y. E.; Headley, J. V. Atmospheric Pressure Photoionization Fourier Transform Ion Cyclotron Resonance Mass Spectrometry Characterization of Oil Sand Process-Affected Water in Constructed Wetland Treatment. *Energy Fuels* **2019**, *33*(5), 4420−4431.

(25) Panda, S. K.; Alawani, N. A.; Lajami, A. R.; Al-Qunaysi, T. A.; Muller, H. Characterization of aromatic hydrocarbons and sulfur heterocycles in Saudi Arabian heavy crude oil by gel permeation chromatography and ultrahigh resolution mass spectrometry. *Fuel* **2019**, *235*, 1420−1426.
(26) Lias, S. G. Ionization energy evaluation in *NIST Chemistry WebBook, NIST Standard Reference Database Number 69*, Linstrom, P.J., Mallard, W.G., Eds.; National Institute of Standards and Technology: Gaithersburg MD, 20899, http://webbook.nist.gov/ (accessed 2020/7/30).
(27) D'Andrilli, J.; Dittmar, T.; Koch, B. P.; Purcell, J. M.; Marshall, A. G.; Cooper, W. T. Comprehensive characterization of marine dissolved organic matter by Fourier transform ion cyclotron resonance mass spectrometry with electrospray and atmospheric pressure photoionization. *Rapid Commun. Mass Spectrom.* **2010**, *24* (5), 643−650.
(28) Podgorski, D. C.; McKenna, A. M.; Rodgers, R. P.; Marshall, A. G.; Cooper, W. T. Selective ionization of dissolved organic nitrogen by positive ion atmospheric pressure photoionization coupled with Fourier transform ion cyclotron resonance mass spectrometry. *Anal. Chem.* **2012**, *84* (11), 5085−5090.
(29) Osborne, D. M.; Podgorski, D. C.; Bronk, D. A.; Roberts, Q.; Sipler, R. E.; Austin, D.; Cooper, W. T. . Molecular-level characterization of reactive and refractory dissolved natural organic nitrogen compounds by atmospheric pressure photoionization coupled to Fourier transform ion cyclotron resonance mass spectrometry. *Rapid Commun. Mass Spectrom.* **2013**, *27*(8), 851−858.
(30) Lusk, M. G.; Toor, G. S.; Inglett, P. W. Characterization of dissolved organic nitrogen in leachate from a newly established and fertilized turfgrass. *Water Res.* **2018**, *131*, 52−61.
(31) Podgorski, D. C.; Corilo, Y. E.; Nyadong, L.; Lobodin, V. V.; Bythell, B. J.; Robbins, W. K.; Rodgers, R. P. Heavy petroleum composition. 5. Compositional and structural continuum of petroleum revealed. *Energy Fuels* **2013**, *27*(3), 1268−1276.
(32) Chacón-Patiño, M. L.; Rowland, S. M.; Rodgers, R. P. Advances in asphaltene petroleomics. part 1: asphaltenes are composed of abundant island and archipelago structural motifs. *Energy Fuels* **2017**, *31* (12), 13509−13518.
(33) Zark, M.; Dittmar, T. Universal molecular structures in natural dissolved organic matter. *Nat. Commun.* **2018**, *9* (1), 1−8.
(34) Witt, M.; Fuchser, J.; Koch, B. P. Fragmentation studies of fulvic acids using collision induced dissociation Fourier transform ion cyclotron resonance mass spectrometry. *Anal. Chem.* **2009**, *81* (7), 2688−2694.
(35) Cortés-Francisco, N.; Caixach, J. Fragmentation studies for the structural characterization of marine dissolved organic matter. *Anal. Bioanal. Chem.* **2015**, *407* (9), 2455−2462.
(36) Zark, M.; Christoffers, J.; Dittmar, T. Molecular properties of deep-sea dissolved organic matter are predictable by the central limit theorem: evidence from tandem FT-ICR-MS. *Mar. Chem.* **2017**, *191*, 9−15.
(37) Polfer, N. C.; Valle, J. J.; Moore, D. T.; Oomens, J.; Eyler, J. R.; Bendiak, B. Differentiation of isomers by wavelength-tunable infrared multiple-photon dissociation-mass spectrometry: application to glucose-containing disaccharides. *Anal. Chem.* **2006**, *78* (3), 670−679.
(38) Brown, T. A.; Jackson, B. A.; Bythell, B. J.; Stenson, A. C. Benefits of multidimensional fractionation for the study and characterization of natural organic matter. *Journal of Chromatography A* **2016**, *1470*, 84−96.
(39) Wagner, S.; Riedel, T.; Niggemann, J.; Vähätalo, A. V.; Dittmar, T.; Jaffé, R. Linking the molecular signature of heteroatomic dissolved organic matter to watershed characteristics in world rivers. *Environ. Sci. Technol.* **2015**, *49* (23), 13798−13806.
(40) Drake, T. W.; Podgorski, D. C.; Dinga, B.; Chanton, J. P.; Six, J.; Spencer, R. G. Land-use controls on carbon biogeochemistry in lowland streams of the Congo Basin. *Global Change Biology* **2020**, *26* (3), 1374−1389.
(41) Spencer, R. G.; Kellerman, A. M.; Podgorski, D. C.; Macedo, M. N.; Jankowski, K.; Nunes, D.; Neill, C. Identifying the Molecular Signatures of Agricultural Expansion in Amazonian Headwater Streams. *J. Geophys. Res.: Biogeosci.* **2019**, *124* (6), 1637−1650.
(42) Luzius, C.; Guillemette, F.; Podgorski, D. C.; Kellerman, A. M.; Spencer, R. G. Drivers of dissolved organic matter in the vent and major conduits of the world's largest freshwater spring. *J. Geophys. Res.: Biogeosci.* **2018**, *123* (9), 2775−2790.
(43) Sleighter, R. L.; Chin, Y. P.; Arnold, W. A.; Hatcher, P. G.; McCabe, A. J.; McAdams, B. C.; Wallace, G. C. Evidence of incorporation of abiotic S and N into prairie wetland dissolved organic matter. *Environ. Sci. Technol. Lett.* **2014**, *1* (9), 345−350.
(44) Lu, Y.; Li, X.; Mesfioui, R.; Bauer, J. E.; Chambers, R. M.; Canuel, E. A.; Hatcher, P. G. Use of ESI-FTICR-MS to characterize dissolved organic matter in headwater streams draining forest-dominated and pasture-dominated watersheds. *PLoS One* **2015**, *10* (12), 1−21.
(45) Mesfioui, R.; Love, N. G.; Bronk, D. A.; Mulholland, M. R.; Hatcher, P. G. Reactivity and chemical characterization of effluent organic nitrogen from wastewater treatment plants determined by Fourier transform ion cyclotron resonance mass spectrometry. *Water Res.* **2012**, *46* (3), 622−634.
(46) Hertkorn, N.; Frommberger, M.; Witt, M.; Koch, B. P.; Schmitt-Kopplin, P.; Perdue, E. M. Natural organic matter and the event horizon of mass spectrometry. *Anal. Chem.* **2008**, *80* (23), 8908−8919.
(47) Hockaday, W. C.; Purcell, J. M.; Marshall, A. G.; Baldock, J. A.; Hatcher, P. G. Electrospray and photoionization mass spectrometry for the characterization of organic matter in natural waters: a qualitative assessment. *Limnol. Oceanogr.: Methods* **2009**, *7* (1), 81−95.
(48) Averett, R. C.; Leenheer, J. A.; McKnight, D. M.; Thorn, K. A.; *Humic substances in the Suwannee River, Georgia; interactions, properties, and proposed structures* (No. 2373). USGPO; US Geological Survey, Map Distribution. 1994
(49) Chebud, Y.; Naja, G. M.; Rivero, R. Phosphorus run-off assessment in a watershed. *J. Environ. Monit.* **2011**, *13* (1), 66−73.
(50) Assegid, Y.; Melesse, A. M.; Naja, G. M. Spatial relationship of groundwater−phosphorus interaction in the Kissimmee river basin, South Florida. *Hydrological Processes* **2015**, *29* (6), 1188−1197.
(51) Aiken, G.; McKnight, D. M.; Thorn, K. A.; Thurman, E. M. Isolation of hydrophilic organic acids from water using nonionic macroporous resins. *Org. Geochem.* **1992**, *18* (4), 567−573.
(52) Cao, X.; Aiken, G. R.; Butler, K. D.; Huntington, T. G.; Balch, W. M.; Mao, J.; Schmidt-Rohr, K. Evidence for major input of riverine organic matter into the ocean. *Org. Geochem.* **2018**, *116*, 62−76.
(53) Aiken, G.; McKnight, D.; Harnish, R.; Wershaw, R. Geochemistry of aquatic humic substances in the Lake Fryxell Basin. *Biogeochemistry* **1996**, *34* (3), 157−188.
(54) Green, N. W.; Perdue, E. M.; Aiken, G. R.; Butler, K. D.; Chen, H.; Dittmar, T.; Stubbins, A. An intercomparison of three methods for the large-scale isolation of oceanic dissolved organic matter. *Mar. Chem.* **2014**, *161*, 14−19.
(55) Poulin, B. A.; Ryan, J. N.; Nagy, K. L., Stubbins, A.; Dittmar, T.; Orem, W.; Aiken, G. R. Spatial dependence of reduced sulfur in Everglades dissolved organic matter controlled by sulfate enrichment. *Environ. Sci. Technol.* **2017**, *51*(7), 3630−3639.
(56) Weishaar, J. L.; Aiken, G. R.; Bergamaschi, B. A.; Fram, M. S.; Fujii, R.; Mopper, K. Evaluation of specific ultraviolet absorbance as an indicator of the chemical composition and reactivity of dissolved organic carbon. *Environ. Sci. Technol.* **2003**, *37* (20), 4702−4708.
(57) Dittmar, T.; Koch, B.; Hertkorn, N.; Kattner, G. A simple and efficient method for the solid-phase extraction of dissolved organic matter (SPE-DOM) from seawater. *Limnol. Oceanogr.: Methods* **2008**, *6* (6), 230−235.
(58) Kaiser, N. K.; Quinn, J. P.; Blakney, G. T.; Hendrickson, C. L.; Marshall, A. G. A novel 9.4 T FTICR mass spectrometer with improved sensitivity, mass resolution, and mass range. *J. Am. Soc. Mass Spectrom.* **2011**, *22* (8), 1343−1351.
(59) Smith, D. F.; Podgorski, D. C.; Rodgers, R. P.; Blakney, G. T.; Hendrickson, C. L. 21 T FT-ICR mass spectrometer for ultrahigh-

resolution analysis of complex organic mixtures. *Anal. Chem.* **2018**, *90* (3), 2041−2047.
(60) Blakney, G. T.; Hendrickson, C. L.; Marshall, A. G. Predator data station: a fast data acquisition system for advanced FT-ICR MS experiments. *Int. J. Mass Spectrom.* **2011**, *306* (2−3), 246−252.
(61) Savory, J. J.; Kaiser, N. K.; McKenna, A. M.; Xian, F.; Blakney, G. T.; Rodgers, R. P.; Marshall, A. G. Parts-per-billion Fourier transform ion cyclotron resonance mass measurement accuracy with a "walking" calibration equation. *Anal. Chem.* **2011**, *83*(5), 1732−1736.
(62) Corilo, Y. E. PetroOrg software. *Florida State University; All Rights reserved.*, 2014; http://www.petroorg.com.
(63) Wickham, H. ggplot2: elegant graphics for data analysis; Springer, 2016.
(64) Larsson, J. eulerr: Area-Proportional Euler and Venn Diagrams with Ellipses. R package version 4.1.0, 2018; https://cran.r-project.org/package=eulerr.
(65) Koch, B. P.; Dittmar, T. From mass to structure: An aromaticity index for high-resolution mass data of natural organic matter. *Rapid Commun. Mass Spectrom.* **2006**, *20* (5), 926−932.
(66) Koch, B. P.; Dittmar, T. From mass to structure: An aromaticity index for high-resolution data of natural organic matter. *Rapid Commun. Mass Spectrom.* **2016**, *30* (1), 250.
(67) Mann, B. F.; Chen, H.; Herndon, E. M.; Chu, R. K.; Tolic, N.; Portier, E. F.; Graham, D. E. Indexing permafrost soil organic matter degradation using high-resolution mass spectrometry. *PLoS One* **2015**, *10*(6), 1−16.
(68) Kassambara, A.; Mundt, F. Factoextra: extract and visualize the results of multivariate data analyses. *R package version* **2017**, *1* (4), 2017.
(69) Hughey, C. A.; Hendrickson, C. L.; Rodgers, R. P.; Marshall, A. G.; Qian, K. Kendrick mass defect spectrum: a compact visual analysis for ultrahigh-resolution broadband mass spectra. *Anal. Chem.* **2001**, *73* (19), 4676−4681.
(70) Riedel, T.; Zark, M.; Vähätalo, A. V.; Niggemann, J.; Spencer, R. G.; Hernes, P. J.; Dittmar, T. Molecular signatures of biogeochemical transformations in dissolved organic matter from ten world rivers. *Frontiers in Earth Science* **2016**, *4*, 85.
(71) Kamjunke, N.; Hertkorn, N.; Harir, M.; Schmitt-Kopplin, P.; Griebler, C.; Brauns, M.; Herzsprung, P. Molecular change of dissolved organic matter and patterns of bacterial activity in a stream along a land-use gradient. *Water Res.* **2019**, *164*, 114919.
(72) D'Andrilli, J.; Cooper, W. T.; Foreman, C. M.; Marshall, A. G. An ultrahigh-resolution mass spectrometry index to estimate natural organic matter lability. *Rapid Commun. Mass Spectrom.* **2015**, *29* (24), 2385−2401.
(73) Hertkorn, N.; Benner, R.; Frommberger, M.; Schmitt-Kopplin, P.; Witt, M.; Kaiser, K.; Hedges, J. I. Characterization of a major refractory component of marine dissolved organic matter. *Geochim. Cosmochim. Acta* **2006**, *70*(12), 2990−3010.
(74) Perminova, I. V.; Dubinenkov, I. V.; Kononikhin, A. S.; Konstantinov, A. I.; Zherebker, A. Y.; Andzhushev, M. A.; Popov, I. A. Molecular mapping of sorbent selectivities with respect to isolation of Arctic dissolved organic matter as measured by Fourier transform mass spectrometry. *Environ. Sci. Technol.* **2014**, *48*(13), 7461−7468.
(75) Dvorski, S. E. M.; Gonsior, M.; Hertkorn, N.; Uhl, J.; Müller, H.; Griebler, C.; Schmitt-Kopplin, P. Geochemistry of dissolved organic matter in a spatially highly resolved groundwater petroleum hydrocarbon plume cross-section. *Environ. Sci. Technol.* **2016**, *50* (11), 5536−5546.
(76) McKnight, D. M.; Boyer, E. W.; Westerhoff, P. K.; Doran, P. T.; Kulbe, T.; Andersen, D. T. Spectrofluorometric characterization of dissolved organic matter for indication of precursor organic material and aromaticity. *Limnol. Oceanogr.* **2001**, *46* (1), 38−48.
(77) Hernes, P. J.; Benner, R. Transport and diagenesis of dissolved and particulate terrigenous organic matter in the North Pacific Ocean. *Deep Sea Res., Part I* **2002**, *49* (12), 2119−2132.
(78) Johnston, S. E.; Striegl, R. G.; Bogard, M. J.; Dornblaser, M. M.; Butman, D. E.; Kellerman, A. M.; Spencer, R. G. Hydrologic connectivity determines dissolved organic matter biogeochemistry in northern high-latitude lakes. *Limnol. Oceanogr.* **2020**, *651764*−1780.
(79) Spencer, R. G.; Mann, P. J.; Dittmar, T.; Eglinton, T. I.; McIntyre, C.; Holmes, R. M.; Stubbins, A. Detecting the signature of permafrost thaw in Arctic rivers. *Geophys. Res. Lett.* **2015**, *42*(8), 2830−2835.
(80) Maizel, A. C.; Remucal, C. K. The effect of advanced secondary municipal wastewater treatment on the molecular composition of dissolved organic matter. *Water Res.* **2017**, *122*, 42−52.

https://dx.doi.org/10.1021/acs.est.0c05206
Environ. Sci. Technol. 2020, 54, 16249−16259